IEPC-95-22

SIMPLE ESTIMATION OF THE PERFORMANCE OF A LOW POWER ARCJET THRUSTER

MICHIO NISHIDA* and HIROYUKI OKAMOTO†

Abstract

This paper describes simple estimation of performance of a low power arcjet thruster using a one-dimensional flow model. Discharge power is put into propellant gas as heat input and then total enthalpy of the propellant gas is increased. In this paper, it is considered that the discharge power is employed not only for elevation of the propellant gas temperature but also for ionization of it. Estimations were carried out for conditions of previously conducted experiment and fairly good agreement between the present calculation and the experiment has been obtained.

Introduction

For the design of arcjet thrusters, it is needed to calculate the flowfield inside the thruster for specified thruster geometry and to predict the performance characteristics of the thruster. This is done generally by numerical calculations using the axisymmetric Navier-Stokes equations coupled with nonequilibrium species mass conservation equations and electric field equations (Ohm's law and Ampère's law), which needs very long computation time to obtain steady state solutions [1]. Therefore, in certain cases, numerical calculations are inconvenient as practical design tools. Nothing would be better than quasi one-dimensional calculation, if that could give satisfactory results to the thruster design. On the view of this point, quasi one-dimensional calculations which are available as simple design tool have been tried and the results have been compared with previous experiments [2].

Flow Model

A flow inside a thruster nozzle is treated as quasi one-dimensional and argon is considered as propellant gas. As shown in Fig. 1, the thruster is divided into four parts as follows:

1. The propellant gas flow is isentropic from the reservoir (0) to the discharge section (1). The flow is calculated by the isentropic relation.

2. A discharge section (1-2) is expressed by a discontinuous plane, and 1 and 2 denote the states immediately ahead and behind the discharge plane, respectively. In this discharge section, the propellant gas is heated by ηVJ, where V is the arc voltage, J is the arc current and η is the efficiency, and at the same time ionization equilibrium is instantaneously established. Thus, the energy input is employed not only for an increase in propellant gas temperature but also for ionization.

3. The propellant gas flow from the discharge section (2) to the throat ($*$) is chemically frozen. The flow in this region is solved using the isentropic relations.

4. The gas is isentropically expanded and aerodynamically accelerated from the throat ($*$) to nozzle exit (e). The flow in this section is solved by the isentropic expansion relations.

*Department of Aeronautics and Astronautics, Kyushu University, Fukuoka 812-81, Japan

†Department of Aeronautics and Astronautics, Kyushu University, Fukuoka 812-81, Japan; Present address, Space System Department, Mitsubishi Electric Corporation, Kamakura 247, Japan

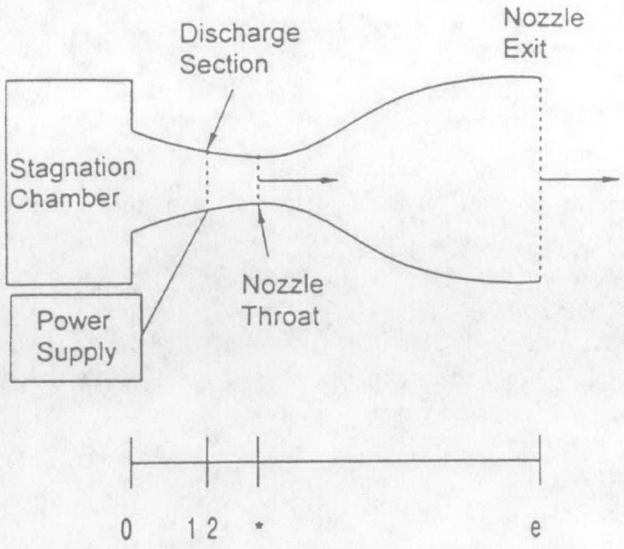

Figure 1: Thruster Model.

Calculation of Flow

The following conservation equations of mass, momentum and energy hold for the flow across the entrance (1) and exit (2) of the discharge section:

$$\rho_1 u_1 = \rho_2 u_2 \tag{1}$$

$$\rho_1 u_1^2 + p_1 = \rho_2 u_2^2 + p_2 \tag{2}$$

$$\dot{m} H_{01} + \eta V J = \dot{m} H_{02} \tag{3}$$

where ρ is the density, u is the velocity, p is the pressure, H_0 is the total enthalpy, $\dot{m}$ is the mass flow rate, η is the efficiency for heating propellant gas. Using Eqs. (1) and (2), we have

$$\frac{p_2}{p_1} = \frac{1+\gamma_1 M_1^2}{1+\gamma_2 M_2^2} \tag{4}$$

$$\frac{\rho_2}{\rho_1} = \frac{u_1}{u_2} = \frac{\gamma_1 M_1^2 (1+R_2 M_2^2)}{\gamma_2 M_2^2 (1+R_1 M_1^2)} \tag{5}$$

Using

$$T_{02} = T_2 \left(1 + \frac{\gamma_2 - 1}{2} M_2^2\right) \tag{6}$$

we have

$$\frac{T_{01}}{T_{02}} = \frac{R_1 \gamma_2 M_2^2 (1+\gamma_1 M_1^2)^2 \left(1 + \frac{\gamma_2 - 1}{2} M_2^2\right)}{R_2 \gamma_1 M_1^2 (1+\gamma_2 M_2^2)^2 \left(1 + \frac{\gamma_1 - 1}{2} M_1^2\right)} \tag{7}$$

where R is the gas constant and γ is the ratio of specific heats, Total enthalpy at the exit of the discharge section is written as

$$H_{02} = C_{p,2} T_{02} + C_i \bar{E}_I \tag{8}$$

where C_p is the specific heat at constant pressure, C_i is the mass fraction of ion and E_I is the ionization energy. From Eqs. (3) and (8),

$$\dot{m}H_{01} + \eta P - \dot{m}C_i E_I = \dot{m}C_{p.2}T_{02} \tag{9}$$

where P denotes the arc power. Conditions at the entrance of the discharge section and arc power are specified, and then T_{02}, T_2, M_2, ρ_2, u_2, p_2, $C_{i.2}$ are obtained using Eqs. (4) to (7), Eq.(9), equation of state and Saha equilibrium relation. Calculations are done with iteration as follows:

1. The value of $C_{i.2}$ is assumed. Initially $C_{i.2} = 0$ is set.
2. Stagnation temperature T_{02} is obtained from Eq. (9).
3. Mach number M_2 is estimated from Eq. (7).
4. p_2, ρ_2 (also u_2) and T_2 are obtained from Eqs. (4), (5) and (6), respectively.
5. $C_{i.2}$ is obtained from Saha equilibrium calculation using T_2 and ρ_2.
6. Steps 2 to 5 are repeated until solutions are converged.

We consider that ionization-recombination is frozen downstream of the discharge section and hence gas constant, specific heat and ratio of specific heats are set to constants. Therefore, since the flow from the discharge section to nozzle throat is treated as isentropic. All properties at the entrance of the discharge section (properties with subscript 1) cannot be specified because a subsonic flow is assumed there. Temperature and mass flow rate are specified at the entrance of the discharge section and other properties (density nad pressure) are determined so as to satisfy the sonic conditions at the throat. Pproperties at the nozzle exit can be determined by using quasi one dimensional nozzle flow equations.

Using quantities at the nozzle exit, performance characteristics of a thruster can be determined as follows:

$$\text{Thrust} : F = \dot{m}u_e \tag{10}$$

$$\text{SpecificImpulse} : I_{sp} = F/\dot{m}g \tag{11}$$

$$\text{efficiency} : \frac{\frac{1}{2}\dot{m}u_e^2}{\dot{m}C_{p1}T_{01} + P} \tag{12}$$

Discharge current is expressed by

$$J = 2\pi r_2 \sigma_2 V \tag{13}$$

where r_2 is the radius at the discharge section and σ_2 is the electric conductivity at the exit of the discharge section. Using Eq.(13), arc current and arc voltage are determined as follows:

$$J = \sqrt{2\pi r_2 \sigma_2 P} \tag{14}$$

$$V = J/2\pi r_2 \sigma_2 \tag{15}$$

The electrical conductivity appearing in Eq.(14) is given by Spitzer's free path theory [3]:

$$\sigma = \frac{3.05 \times 10^{-12} n_e}{\sqrt{T}\sum_j n_j Q_{ej}} \quad \text{mho/m.} \tag{16}$$

In Eq. (16), n_j denotes the number density of species j and Q_{ej} is the collision cross section for electron-species j encounters

$$Q_{ea} = (0.39 - 0.551 \times 10^{-4}T + 0.595 \times 10^{-8}T^2) \times 10^{-20}\text{m}^2 \quad \text{for } T < 10^4\text{K} \tag{17}$$

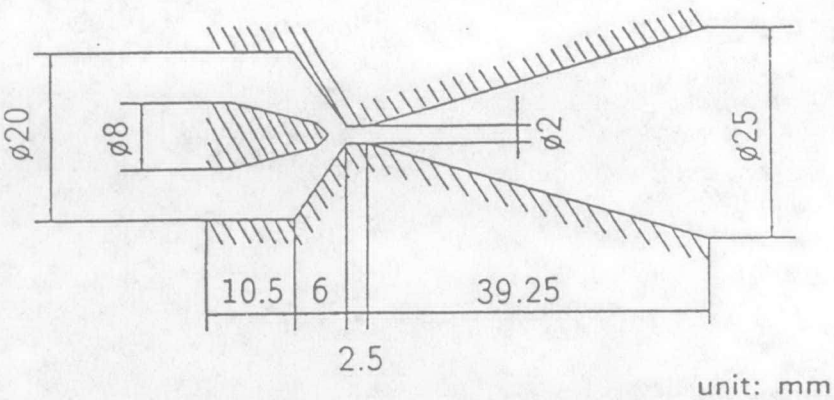

Figure 2: Thruster Geometry.

$$Q_{ea} = (-0.35 + 0.775 \times 10^{-4}T) \times 10^{-20}\mathrm{m}^2 \quad \text{for } T > 10^4\mathrm{K} \tag{18}$$

$$Q_{ei} = \frac{5.85 \ln \Lambda}{T^2} \times 10^{-20}\ \mathrm{m}^2 \tag{19}$$

$$Q_{ee} = 0.707 Q_{ei}\ \mathrm{m}^2, \tag{20}$$

where

$$\Lambda = \frac{1.24 \times 10^7 T^{3/2}}{\sqrt{n_e}}, \tag{21}$$

and the subscripts ea, ei, and ee denote the electron-atom, electron-ion and electron-electron encounters, respectively.

Results

First of all, the effect of a diameter in the discharge section upon the performance characteristics of a thruster was investigated. The conditions considered are

Mass flow rate: 0.1g/s
Temperature at the entrance of the discharge section: $T_1 = 300$K
Arc power: $P = 1$kw
Efficiency: $\eta = 0.5$
Nozzle throat diameter: 2.0mm
Nozzle exit diameter: 25mm.

Calculations were carried out for two different diameters at the discharge section, i.e., d =2.1mm and 7.0mm. Calculated temperature at the discharge section (T_2), degree of ionization at the discharge section (α_2), propulsion efficiency (η_{prop}), thrust(F), specific impulse (I_{sp}), arc voltage (V) and arc current (J) are shown in Table 1.

It is seen from the table that in case of smaller diameter, the propulsion efficiency, thrust and specific impulse are increased compared with those for larger diameter.

The analysis has been conducted for the same thruster nozzle geometry as used in the experiments (see Fig. 2). The diameter at the discharge was set to 7mm, which was determined from the cathode geometry. The efficiency was set to 0.5, which includes the heat loss due to radiation cooling and nozzle viscous loss. Figure 3 shows results for thrust and comparisons with previous numerical data [1] and experiments [2]. The present result shows that the thrust is increased with mass flow rate. Numerical results and experimental ones

are similar to the present ones, and hence it may be mentioned that the present results are in fairly good agreements with the numerical simulation and experiments though the analysis is very simple.

The results for specific impulse are illustrated in Fig. 4. The present result shows that specific impulse is decreased with mass flow rate. The numerical calculations and experiments also give similar results and fairly satisfactory agreements also are obtained.

References

[1] H. Okamoto, M. Nishida, K. Tanaka and A. Beylich, "Numerical Simulation of the Performance of a Radiation-cooled 1kw DC Arcjet Thruster", Proc. 23rd Int. Electric Propulsion Conf., Seattle, pp.1655-1661 (1993).

[2] K. Tanaka, K. Tsuchiya, K. Kaita and M. Nishida, "Experimental Investigation on the Characteristics of a Low Power DC Arcjet Thruster", Proc. 20th Int. Electric Propulsion Conf., Garmisch-Partenkirchen, FRG, pp.620-626 (1988).

[3] A.B. Cambel, Plasma Physics and Magnetofluidmechanics, McGraw-Hill, New York, pp.152-191 (1963).

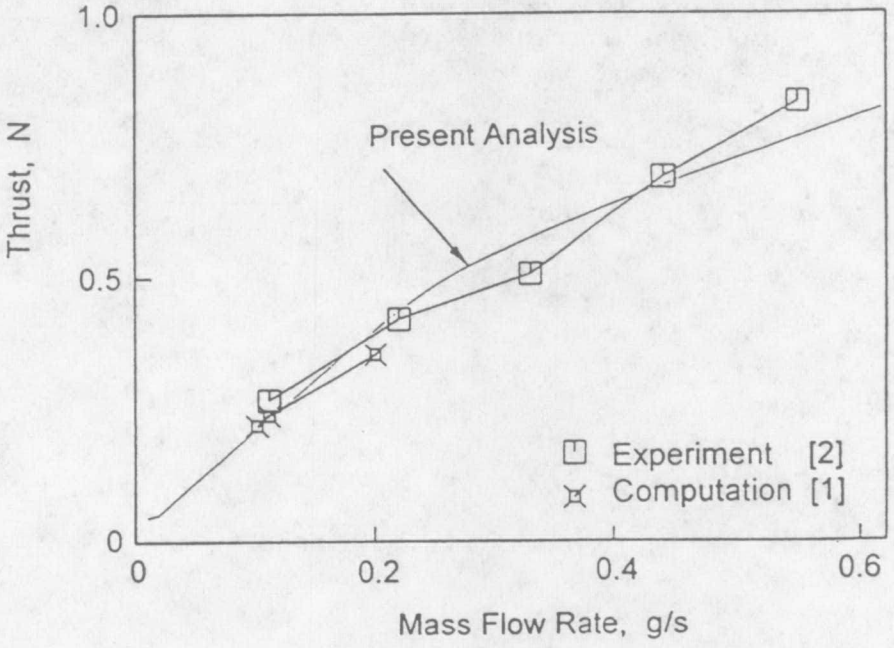

Figure 3: Thrust vs Mass Flow Rate

Table 1: Performance characteristics of a thruster for two different diameters of the discharge section.

d	T_2	α_2	η_{prop}	F	I_{sp}	V	J
2.1mm	4680K	5.8%	29.0%	242mN	247s	24volt	40amp
7.0mm	4510K	7.0%	24.0%	223mN	227s	15volt	66amp

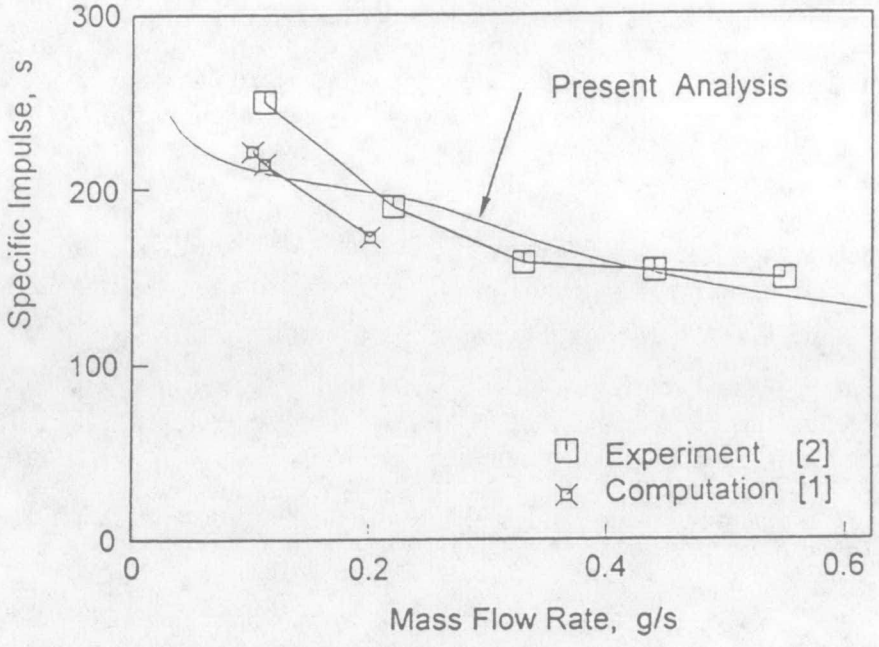

Figure 4: Specific Impulse vs Mass Flow Rate